Analytical Estimate for Curing-Induced Stress and Warpage in Coating Layers

K. M. B. Jansen, J. de Vreugd, L. J. Ernst

Product Engineering Section, Department of Design Engineering, Delft University of Technology, The Netherlands

Received 15 December 2011; accepted 23 December 2011
DOI 10.1002/app.36776
Published online in Wiley Online Library (wileyonlinelibrary.com).

ABSTRACT: A thermoset coating that is applied to an elastic substrate will develop residual stresses during curing because of polymerization shrinkage of the resin. This shrinkage only partly contributes to the residual stresses because, before gelation, the stresses relax completely. In this study, we developed explicit analytical expressions for the curing efficiency factor, the residual stresses, and the resulting warpage. We did this by assuming that after gelation, the material was in its rubbery state and that viscoelastic effects were absent. A difference between the free and constrained warpages during curing was made. The analytical warpage models were shown to give results comparable to those of the numerical calculations with a fully curing-dependent viscoelastic material model. Furthermore, for the first time, accurate analytical expressions for the stress-free temperature and stress-free strain were obtained. With these expressions, the effect of curing shrinkage on the residual stresses could easily be incorporated into existing (numerical) stress analysis without the need for extensive curing-dependent viscoelastic material models. © 2012 Wiley Periodicals, Inc. J. Appl. Polym. Sci. 000: 000–000, 2012

Key words: coatings; curing of polymers; resins; stress; thermosets

INTRODUCTION

The construction of bilayered or multilayered plates of arbitrary thickness usually show substantial residual stresses, and if the assemblies are not supported, this will result in warpage. The understanding of these stresses and warpage is of practical importance because residual stresses will have a negative effect on product life and may eventually lead to failure, whereas warpage may cause other problems. An electronic package (a combination of a metal lead frame, a chip, and an epoxy coating) that is warped, for example, cannot be soldered to a flat substrate.

The problem of warpage predictions for assemblies of isotropic elastic plates is well known and illustrated in the literature. It started with Stoney,[1] who derived a simple analytical expression for relating the stress in a thin elastic coating on a substrate to the observed curvature. This analysis was later modified to allow for constructions with arbitrary thickness ratios and arbitrary ratios between the coating and substrate moduli. A good overview of this literature was given by Klein.[2] The analysis was extended to cover constructions consisting of more than two layers (e.g., refs. 3, 4 and 5).

Correspondence to: K. M. B. Jansen (k.m.b.jansen@tudelft).

These kind of bilayer and multilayer models are very useful for predicting the warpage caused by differences in thermal expansion of the individual layers. What they cannot do, however, is predict the residual stress and corresponding warpage related to the application process of the coating layer itself; that is, they cannot predict the curing-induced warpage. Consider, for example, a metal strip on which a thin layer of thermoset coating is applied at a certain elevated temperature. At this temperature, the resin starts to cure, a process during which it transforms from a liquid to a viscoelastic solid. This curing process is always accompanied by shrinkage. For epoxies, this curing shrinkage is about 3–4%, but for polyester resins, it can be as high as 10%.[6] Because of the combination of this curing shrinkage and the increasing modulus, residual stresses build up and result in curing-induced warpage. Additional stresses and warpage may develop during cooling from the processing temperature to ambient conditions. For these thermal stresses, already good analytical models exist, but models for the curing-induced stresses and warpage do not exist yet.

The warpage of thermoset layers due to processing at elevated temperatures can be considered to consist of two parts: stresses formed during the relatively short curing stage and stresses that occur during the cooling afterward. One can demonstrate the existence of curing-induced stresses simply by heating a warped structure and observing the change in the curvature. The temperature at which the

curvature disappears is referred to as the *stress-free temperature*, and the fact that this occurs above the curing temperature already shows that residual stresses due to curing must be present. Another example of the existence of curing-induced stresses are the fractures that sometimes occur when fragile (optical) components are glued to rigid substrates with a room-temperature-curable adhesive. For thermosets cured at higher temperatures, the thermal shrinkage is about 1% (for the cooling of a material with a coefficient of thermal expansion of 70 ppm/K over a range of 150 K); this is the same order of magnitude as the curing shrinkage (2% linear shrinkage, which is, e.g., 50% effective). Both contributions should, therefore, in principle be considered in any stress analysis. In practice, however, the curing-induced stress part is often neglected[6] or, at best, taken into account with an adjustable stress-free temperature[7–10] or initial strain contribution.[11,12] In all these articles, the stress-free temperature and strain were used as empirical fit parameters to match simulation results to the experimental warpage. In that way, reasonable estimates of the residual stress distributions in a series of similar products could be obtained. However, the *a priori* prediction of warpage of new substrate-coating combinations was not possible with that approach.

In this study, we developed an analytical model for predicting the stress-free temperature and strain and the curing-induced warpage of bilayer structures. This is relevant not only for the field of coating technology but also for the field of microelectronics. Because of the extremely high production volumes and a strong need for cost reduction, this field of industry strives toward a very low failure rate. A good knowledge of residual stresses and warpage is, therefore, indispensable. Recently, much effort has been put into the characterization of the change in material properties during curing[13] and the numerical implementation of these material models.[14]

ANALYSIS

Warpage of a bilayer structure without curing

For simplicity, we repeat here the stress analysis of bilayer structures in which the elastic properties do not change (e.g., ref. 2 and references therein). This starts with the consideration of a structure consisting of two bonded layers, each of which is subjected to an initial strain (ε_i^0). The initial strain is usually the thermal expansion strain ($\varepsilon_i^{0,T} = \alpha_i \Delta T$, where α_i is the coefficient of thermal expansion of layer i and ΔT is the change in temperature). The initial strain, however, can also be of a different origin (i.e., strains due to the deposition of additional layers or, as we see later, chemical shrinkage during thermoset curing). We assume that the layers are elastic and that the strains are isotropic and uniform through the thickness. These strains generate biaxial in-plane stresses (σ_i's):

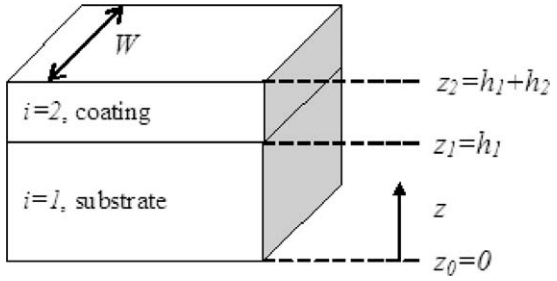

Figure 1 Schematic diagram of the two-layer structure.

$$\sigma_i = \frac{E_i}{1-\nu_i}\left[\varepsilon_i - \varepsilon_i^0\right] \tag{1}$$

where E_i, ν_i, and ε_i denote the elastic modulus, Poisson ratio, and strain of layer i. The strain in each layer consists of a planar strain ($\bar{\varepsilon}$), which is identical for both layers, and a bending contribution [$\kappa(z - z_b)$, where κ is the curvature, z is the thickness coordinate, and z_b is the neutral plane]:

$$\varepsilon_i = \bar{\varepsilon} + \kappa(z - z_b) \tag{2}$$

Because of the initial strains, the structure will expand and warp, and this can be calculated by a simple assumption of equilibrium of forces (F_i's) and moments (M_i's):

$$F_1 + F_2 = W\int_0^{h_1}\sigma_1 dz + W\int_{h_1}^{h_1+h_2}\sigma_2 dz = 0 \tag{3}$$

$$M_1 + M_2 = W\int_0^{h_1} z\sigma_1 dz + W\int_{h_1}^{h_1+h_2} z\sigma_2 dz = 0 \tag{4}$$

where W is the sample width (see Fig. 1). For practical reasons, we introduce the dimensionless thickness ($a = h_2/h_1$, with h_1 and h_2 being the thickness of layer 1 and 2 respectively) and the modulus ratio ($b = E_2'/E_1'$, where E_i' denotes the reduced modulus $E/(1 - v)$ of layer i). By combining the first three equations, we can solve for the planar strain and neutral plane and get[2]

$$\bar{\varepsilon}/h_1 = \frac{\varepsilon_1^0 + ab\varepsilon_2^0}{1+ab}, \qquad z_b/h_1 = \frac{\frac{1}{2}[1 + a(a+2)b]}{1+ab}. \tag{5}$$

We can then find the curvature by inserting this into Eq. (4) and solving for κ:

$$\kappa = \frac{6a(a+1)b}{h_1 N}\left[\varepsilon_2^0 - \varepsilon_1^0\right] \quad (6)$$

where N is defined as

$$N = 1 + b\left(4a^3 + 6a^2 + 4a\right) + b^2a^4.$$

This is the well-known bending equation for structures consisting of two elastic layers with arbitrary initial strains.[2,15] For thin coating layers ($a \ll 1$), the equation is considerably simpler and leads to what is known as the Stoney equation for thermal strains[1]:

$$\kappa = \frac{6ab}{h_1}\Delta\alpha\Delta T.$$

where $\Delta\alpha$ is the difference in coefficients of thermal expansion. In practice, warpage is often expressed as the vertical deflection (bow) of a curved plate put onto a flat surface. Simple geometrical considerations then lead to the following relation between the curvature and deflection (d):

$$d = R[1 - \cos(2L/R)] \cong \tfrac{1}{8}L^2\kappa, \quad (7)$$

where L is the length of the bimaterial strip and R is the radius of the curvature ($R = 1/\kappa$).

In this study, we defined expansion as positive and shrinkage as negative. Therefore, a positive curvature corresponded to the expansion of layer 2 and was toward the substrate layer. The residual stresses in each layer could be found by the combination of eqs. (1), (2), (5), and (6).

Bilayer warpage with curing shrinkage and modulus increase

The next step is to include the effect of curing on warpage. This is complicated by the fact that during curing, not only does the intrinsic strain in the coating layer (ε_2^0) change but its modulus (E_2) also does. Initially, the coating is liquidlike, and the curing shrinkage after each incremental time step does not result in a stress increase. However, if the coating polymerizes beyond what is called the *gel point*, the polymer starts to form a three-dimensional network structure in which mechanical stress can pertain. An increase in the curing shrinkage now causes a small stress, which partially relaxes because of the viscoelastic nature of the incomplete polymer network. During the next time step, the same amount of chemical shrinkage results in a larger stress buildup, followed by a smaller stress relaxation. This process of stress buildup and relaxation continues until the polymer layer is fully cured.

It is clear that the previous process is difficult for one to evaluate further without making simplifications. Therefore, we restricted ourselves to thermosets that cured above their final glass-transition temperature and assumed that the dominating effect would be from the combination of progressing curing shrinkage and modulus increase and that viscoelastic effects (stress relaxation) were of less importance. Above the glass transition, the material can be considered to be in its rubber elastic state and $E_2(t,\zeta) \approx E_2(\zeta)$, where ζ is the chemical conversion and t is the time. Such a situation is quite common for thermoset systems because systems that cure at a temperature below their glass transition will vitrify during curing, such that full conversion is never reached. Because we neglected viscoelastic effects, we always evaluated the coating layer in its lowest (equilibrium) stress state, and this approximation underestimated the stress buildup in the coating layer and, thus, also underestimated the warpage of the bilayer assembly. It was, however, expected that the effect of this underestimation would be small.

The analysis of the residual stresses and warpage generated during the curing stage can be done for two types of boundary conditions: freestanding curing and constrained curing. In the first case, the bimaterial strip is free to shrink and warp during the curing stage. This applies, for example, to the curing of a coating layer applied to a thin metal strip. The constrained curing case corresponds to what occurs during the encapsulation of electronic packages.[10–12] During this process, a metal lead frame with a chip is placed in a heated mold, after which the mold is filled with an epoxy resin. During filling and curing, the lead frame is fixed, and warpage is prevented. After mold opening, the assembly is free to warp. We did expect differences between the two cases because, in the case of unconstrained curing, each new gelled layer adheres onto a curved structure and then starts with its shrinkage and stress generation, whereas in the constrained case, each new layer adheres onto the flattened structure. We, thus, expected the free cured structure to show the most warpage.

Free curing analysis

Instead of the total force balance [Eq. (3)], we now consider the incremental increase in force (dF_{tot}) after a small increase in time and evaluate Eq. (3) with $d\sigma_i = E'_i(d\varepsilon_i - d\varepsilon_i^0)$:

$$dF_{tot} = \int_0^{h_1} E'_1\left[d\bar{\varepsilon} - d\varepsilon_1^0 + (z - z_b)d\kappa\right]dz + \int_0^{h_1+h_2} E'_2\left[d\bar{\varepsilon} - d\varepsilon_2^0 + (z - z_b)d\kappa\right]dz = 0 \quad (8)$$

The solution of the incremental midplane strain then gives (with dimensionless thickness and modulus ratios)

$$d\bar{\varepsilon}/h_1 = \frac{d\varepsilon_1^0 + ab(\zeta)d\varepsilon_2^0}{1+ab(\zeta)}, \tag{9}$$

where we used the approximation $d(z_b\kappa) \approx z_b d\kappa$.

For the change in moment (dM), we get

$$E_1'\left[d\bar{\varepsilon} - d\varepsilon_1^0 - z_b d\kappa\right]\tfrac{1}{2}h_1^2 + E_2'\left[d\bar{\varepsilon} - d\varepsilon_2^0 - z_b d\kappa\right] \times \tfrac{1}{2}\left(h_2^2 + 2h_1h_2\right) + d\kappa\left\{\tfrac{1}{3}E_1'h_1^3 + \tfrac{1}{3}E_2'\left(h_2^3 + 3h_2^3h_1 + 3h_2h_1^2\right)\right\} = 0$$

From this, we obtain the desired incremental increase in the curvature ($d\kappa$). After integration, this gives

$$\kappa = \int_0^t \frac{6a(a+1)b}{h_1 N}\left[\dot{\varepsilon}_2^0 - \dot{\varepsilon}_1^0\right]dt,$$

$$N = 1 + b\left(4a^3 + 6a^2 + 4a\right) + b^2a^4 \tag{10}$$

$$\bar{\varepsilon} = \int_0^t \frac{\dot{\varepsilon}_1^0 + ab\dot{\varepsilon}_2^0}{1+ab}dt, \quad z_b = \frac{\frac{1}{2}[1 + a(a+2)b]h_1}{1+ab}, \tag{11}$$

where the dot over the intrinsic strain terms refers to differentiation with respect to time. Note that both the modulus ratio and the intrinsic strains vary with time. For solvent-deposited thermoplastic coatings, the coating layer thickness decreases considerably during solvent evaporation, such that the thickness ratio also should be treated as time dependent. Also essential is the fact that the integration is not just over the modulus–intrinsic strain term [numerator of Eq. (9)] but includes the variation of the terms in the denominator as well. The reason is that after each incremental time step, not only does the modulus and planar strain increase but the neutral position also changes.

To be able to better understand the separate contributions of curing and thermal shrinkage to the curvature and residual stresses, we start by explicitly separating the two contributions in the intrinsic strains (note that the substrate layer only has a thermal shrinkage contribution):

$$\varepsilon_1^0 = \varepsilon_1^{0,T} = \alpha_1\Delta T$$
$$\varepsilon_2^0 = \varepsilon_2^{0,c} + \varepsilon_2^{0,T} = \varepsilon_2^c + \alpha_2\Delta T.$$

where the superscripts "T" and "c" refer to the thermal and curing contributions, respectively

Next, we assume that the curing step is isothermal and that there is no reaction during cooling. Then, we obtain for the curvatures due to thermal and curing contributions

$$\kappa^c = \int_0^\zeta \frac{6a(a+1)b(\zeta)}{h_1N(\zeta)}\frac{d\varepsilon_2^c(\zeta)}{d\zeta}d\zeta, \tag{12}$$

$$\kappa^T = \int_{T_c}^{T_0} \frac{6a(a+1)b(T)}{h_1N(T)}[\alpha_2(T) - \alpha_1(T)]dT. \tag{13}$$

Note that because for the curing-dependent contribution both the curing shrinkage and the relative modulus ratio directly depend on the conversion and only indirectly on time, we used the conversion as the new integration variable. Analogously, for the thermal contribution, we used the temperature as the integration variable. Further simplifications can be obtained by the assumption that the curing shrinkage is linear with respect to conversion [$d\varepsilon_2^c = \varepsilon_{2\max}^c d\zeta$, where $\varepsilon_{2\max}^c$ then denotes the curing shrinkage after full conversion (see Simplifications and Limiting Cases section)].

Constrained curing

Here, we assume that the structure is constrained during the curing process such that both the midplane strain and curvature are suppressed. We, thus, can use Eq. (8) with $d\bar{\varepsilon} = d\kappa = 0$ and obtain for the incremental increase in total force

$$dF_{\text{tot}} = -E_2'(\zeta)h_2 d\varepsilon_2^0$$

where we also assumed that the intrinsic strains in the substrate were absent ($d\varepsilon_1^0 = 0$). The in-plane force at the end of curing is thus

$$F_{\text{end}} = -h_2\int_0^1 E_2'(\zeta)\frac{d\varepsilon_2^0}{d\zeta}d\zeta \tag{14}$$

Note that the changes in the shrinkage strain ($d\varepsilon_2^0$) are negative such that F_{end} is of a tensile nature. This force is balanced by the forces in the mold walls. When the mold opens and the structure is released, it will shrink and warp with the force given by Eq. (14) as the driving force. Denoting $\Delta\bar{\varepsilon}$ and $\Delta\kappa$ as the changes in the in-plane shrinkage and curvature, respectively, and using Eq. (8), we obtain

$$\int_0^{h_1} E_1'[\Delta\bar{\varepsilon} + (z - z_b)\Delta\kappa]dz + \int_0^{h_1+h_2} E_2'[\Delta\bar{\varepsilon} + (z - z_b)\Delta\kappa]dz + F_{\text{end}} = 0.$$

Integration and rearrangement results in

$$\Delta\bar{\varepsilon}[E_1'h_1 + E_2'h_2] + \Delta\kappa[\tfrac{1}{2}(E_1'h_1^2 + E_2'\{h_2^2 + 2h_1h_2\}) - z_b(E_1'h_1 + E_2'h_2)] + F_{\text{end}} = 0.$$

This has to be true independently of $\Delta\kappa$. Thus, the $\Delta\kappa$ term must vanish and

$$\Delta\bar{\varepsilon} = \frac{F_{\text{end}}/E_1' h_1}{1+ab}, \quad z_b = \frac{\frac{1}{2}[1+a(a+2)b]h_1}{1+ab}. \tag{15}$$

Similar to the derivation for the free curing case, we now obtain the warpage from the change in moment:

$$\Delta\kappa^c = -\frac{6a(1+a(a+2)b)}{h_1 N}\int_0^1 b(\zeta)\frac{d\varepsilon_2^c(\zeta)}{d\zeta}d\zeta \tag{16}$$

where $\Delta\kappa^c$ is the warpage change upon ejection. Remember that in Eq. (16), the modulus E_2 in the modulus ratio and N should be evaluated in its (fully cured) rubbery state. The curvature changes due to cooling after ejection are given by Eq. (13). As before, if the curing shrinkage is linear, $d\varepsilon_2^c/d\zeta$ can be replaced with $\varepsilon_{\max}^c$.

Stress-free temperature and strain

A bimaterial strip that is curved after processing can always be heated to such a temperature that the curvature just vanishes. This temperature is then called the *stress-free temperature*, although internally, it is not necessarily free of stress. The stress-free temperature is easy to measure and is, therefore, often used in numerical simulations of cooling stresses as an approximate way to account for the curing-induced stresses we discussed previously. Related to this is what we call the *stress-free strain*, which can be defined as that coating-layer strain that will cause the curing-induced warpage to disappear. Also, this stress-free strain is used as an empirical parameter to take into account the processing-induced stresses in subsequent numerical calculations.[12] Up to this point, no explicit expressions are available that relate these stress-free parameters to the curing-induced shrinkage and modulus increase. For the derivation, we start with the stress-free strain ($\varepsilon_2^{\text{SF}}$) and assume that it is a uniform strain that is confined to the coating layer and that is evaluated at the curing temperature (i.e., thermal stresses are absent). From Eq. (6), it then follows that the curvature equals

$$\kappa = \frac{6a(a+1)b_R\varepsilon_2^{\text{SF}}}{h_1 N_R},$$

where we use the subscript R to indicate that the modulus E_2, and its ratio needs to be evaluated in its rubbery state. Equating this to the curing-induced warpage [Eq. (12)] and assuming the thickness ratio remain constant, we then obtain

$$\varepsilon_2^{\text{SF}} = f_c\varepsilon_2^{c,\max},$$
$$f_c = \frac{1}{\varepsilon_2^{c,\max}}\frac{N_R}{b_R}\int_0^1 \frac{b(\zeta)}{N(\zeta)}\frac{d\varepsilon_2^c}{d\zeta}d\zeta = \frac{N_R}{b_R}\int_0^1 \frac{b(\zeta)}{N(\zeta)}d\zeta. \tag{17}$$

where, in the last step, it is assumed that the curing shrinkage is proportional to the conversion: $\varepsilon_2^c(\zeta) = \varepsilon_2^{c,\max}\zeta$. The curing shrinkage efficiency factor (f_c) is defined as the ratio between the stress-free strain and the maximum curing strain ($\varepsilon_2^{c,\max}$). It is a measure of the efficiency at which the curing shrinkage is transferred to residual stress. If, for example, the coating modulus is zero before gelation and constant after gelation and the conversion at gelation (ζ_{gel}) = 0.40, the efficiency factor would be $f_c = 0.60$. Because the coating modulus is not constant but gradually increases after gelation, the actual efficiency factor is lower. Note that the maximum efficiency factor is given by $f_c^{\max} = 1 - \zeta_{\text{gel}}$. This limit is reached either if the substrate is very thin ($a \gg 1$) or if the coating modulus changes stepwise to its maximum value at the gelation point.

Next, we derive an expression for the stress-free temperature. According to its definition, we must balance the thermal and curing-induced warpage terms such that $\kappa^T + \kappa^c = 0$. With eqs. (12) and (13), we then obtain

$$\int_0^1 \frac{b(\zeta)}{N(\zeta)}\frac{d\varepsilon_2^c}{d\zeta}d\zeta + \int_{T_c}^{T^{\text{SF}}} \frac{b(T)}{N(T)}[\alpha_2 - \alpha_1]dT = 0.$$

where T^{SF} is the stress-free temperature and T_c denotes the curing temperature. Assuming again that the modulus values and the coefficient of thermal expansion are evaluated at their rubbery values and using the expression for the stress-free strain, we get

$$T^{\text{SF}} = T_c - \frac{f_c\varepsilon_2^{c,\max}}{\alpha_2^R - \alpha_1}. \tag{18}$$

here the superscript "R" refers to the rubbery state.

Note that the stress-free temperature is above the curing temperature because $\varepsilon_2^{c,\max}$ is negative, and usually, $\alpha_2^R > \alpha_1$. Typically, the difference is about 20–50°C.

Simplifications and limiting cases

The goal of this section is to derive explicit expressions for limiting cases or for special choices of the modulus and curing shrinkage curves. These explicit expressions are useful for checking the correctness of the implementation in finite element software and to allow for a quick estimate of warpage in a specific case without the need to first setup a numerical model. Therefore, we focus on the effect of curing

shrinkage in the coating layer and evaluate all of the expressions with $\varepsilon_2^{0,T} = \varepsilon_1^{0,T} = 0$. Furthermore, we assume that the curing shrinkage is linear with respect to conversion. This assumption is motivated by the fact that during polymerization, monomers are added step by step to the polymer network. By this process, they lose part of their mobility, and it is, thus, likely that the loss in free volume is proportional to the amount of reacted monomer because the loss in free volume is observed as shrinkage. This leads to

$$\varepsilon_2^c(\zeta) = \varepsilon_2^{c,\max}\zeta, \tag{19}$$

where $\varepsilon_2^{c,\max}$ is the total amount of curing shrinkage. This linear relation has been observed for a number of epoxy systems[16,17] but should not be considered as general.[18] For this purpose, however, we assume Eq. (19) to hold.

Small coating thickness [$h_2 \ll h_1$ ($a \ll 1$)]

If h_2 is small, the average shrinkage and the neutral plane coordinate become [see Eq. (11)]

$$\bar{\varepsilon}(\zeta) = a\varepsilon_2^{c,\max}\int_0^\zeta b(\zeta)d\zeta, \quad z_b = \tfrac{1}{2}h_1, \quad a \ll 1 \tag{20}$$

such that the curvature at conversion becomes

$$\kappa(\zeta) = \frac{6a\varepsilon_2^{c,\max}}{h_1}\int_0^\zeta b(\zeta)d\zeta, \quad a \ll 1. \tag{21}$$

This, thus, allows us to check the curvature predictions for different functions [$b(\zeta)$ or $E_2(\zeta)$]. We start with a constant coating modulus and linearly increasing curing shrinkage [Eq. (19)]. This gives

$$\kappa \approx \frac{6ab_m}{h_1}\varepsilon_2^{c,\max}\zeta, \quad a \ll 1, b = b_m \quad \varepsilon_2^0 = \varepsilon_2^{c,\max}\zeta. \tag{22a}$$

where b_m is a constant.

Verification with $h_1 = 1$ mm, $a = 10^{-2}$, $b_m = 1$, and $\varepsilon_2^{c,\max} = 0.04$ gives $\kappa = 2.4$ m^{-1}, which agrees well with the 2.325 predicted by Eq. (12). For both linear increases in the coating modulus and intrinsic strain, we obtain a quadratic increase in the curvature with ongoing curing:

$$\kappa \approx \frac{6ab_m}{h_1}\varepsilon_2^{c,\max}\tfrac{1}{2}\zeta^2, \quad a \ll 1, b = b_m\zeta, \quad \varepsilon_2^0 = \varepsilon_2^{c,\max}\zeta. \tag{22b}$$

In reality the coating modulus first increases slowly with curing followed by an acceleration toward the end of curing. Therefore, it is more realistic to assume an exponential increase in conversion and obtain

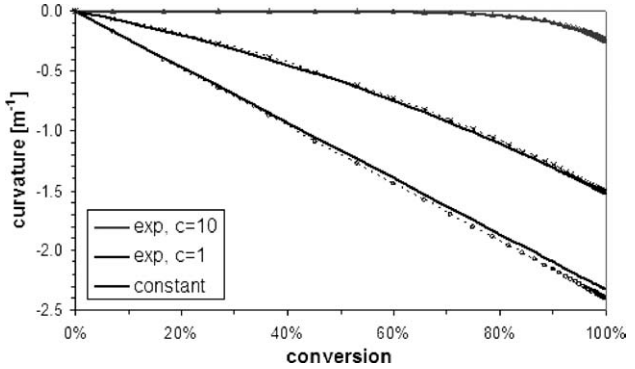

Figure 2 Comparison between the (—) full calculation with Eq. (12) and (- - -) approximations [Eq. (22)]. $h_1 = 1$ mm, $a = 10^{-2}$, $\varepsilon_2^{c,\max} = -0.04$ for cases $b = 1$ and $b = e^{c(\zeta-1)}$.

$$\kappa \approx \frac{6ab_m}{h_1}\frac{\varepsilon_2^{c,\max}}{c}[e^{c(\zeta-1)} - e^{-c}], \quad a \ll 1, b = b_m e^{c(\zeta-1)}, \quad \varepsilon_2^0 = \varepsilon_2^{c,\max}\zeta \tag{22c}$$

where c is a constant. With the data set $h_1 = 1$ mm, $a = 10^{-2}$, $b_m = 1$, $\varepsilon_2^{c,\max} = 0.04$, and $c = 1$, eq. (22c) predicts a final curvature of 1.517 m^{-1}, whereas the full Eq. (12) gives 1.526 m^{-1}. For $c = 10$, these results are 0.240 and 0.245 m^{-1}, respectively. The agreement is good. The corresponding curvature changes during curing are plotted in Figure 2. This shows that for exponential modulus growth, the approximations are better than in the constant-modulus case.

Small substrate thickness ($a \gg 1$, $ab \gg 1$)

If the curing coating layer is deposited or molded on top of a thin, soft substrate, the in-plane contraction of the structure is governed by the shrinkage of the coating layer only, and the curvature is small. The equations then reduce to

$$\bar{\varepsilon} \approx \varepsilon_2^c(\zeta), \quad z_b \approx \tfrac{1}{2}h_2 + h_1, \quad a \gg 1, ab \gg 1. \tag{23}$$

$$\kappa \approx \int_0^\zeta \frac{6\varepsilon_2^{c,\max}}{h_1 a[ab+4]}d(\zeta), \qquad a \gg 1, ab \gg 1. \tag{24}$$

With $a = h_2/h_1$, this shows that the curvature indeed vanishes as h_1 approaches zero.

COMPARISON WITH VISCOELASTIC NUMERICAL SIMULATIONS

The main assumption in this curing-dependent warpage model is that viscoelastic effects are

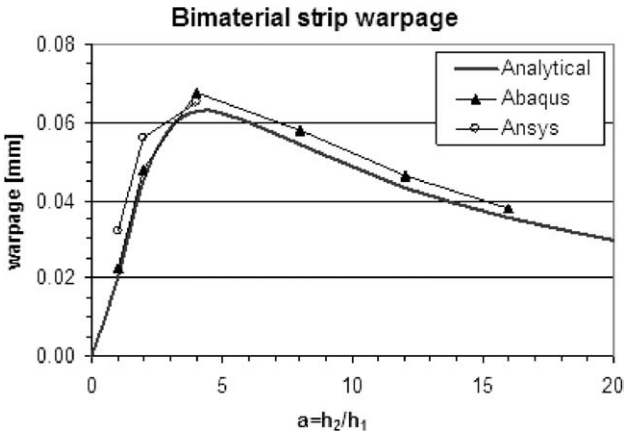

Figure 3 Numerical and analytical deflection of the bilayer strip versus the h_2/h_1 ratio.

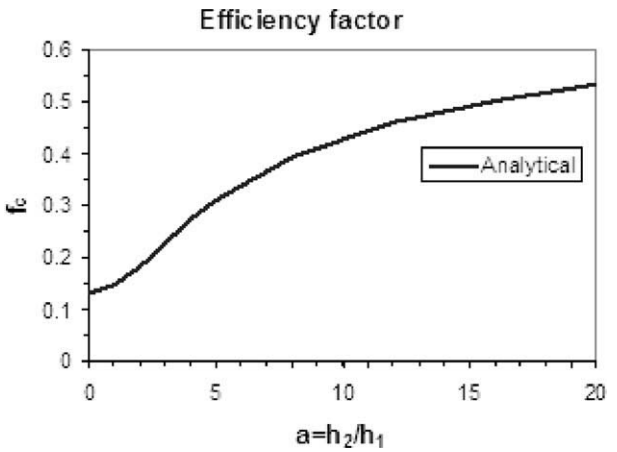

Figure 5 Predicted curing shrinkage efficiency factor [Eq. (17)].

negligible during curing. That means that the stresses in the coating layer are always evaluated with the lowest modulus limit (i.e., in the rubbery state). The stresses and the curvature are, therefore, underestimated. To check the validity of the assumption, warpage predictions from Eq. (12) were compared with numerical simulations involving a fully curing-dependent viscoelastic material model. This curing-dependent model was implemented in both Ansys (Canonburg, Pennsylvania) and Abaqus (Pawtucket, Rhode Island) software with dedicated Fortran subroutines.

As an example, we considered the warpage of a structure consisting of a molding compound used for chip encapsulation and a copper lead frame. The lead frame had a values of $E_1 = 123$ GPa, $\nu_1 = 0.33$, $h_1 = 0.5$ mm, and $\alpha_1 = 17.5\ 10^{-6}$/K. Accurate predictions of the warpage and curing-induced stresses are important in the microelectronics industry because they are seen as one of the main causes for product failure. We, therefore, took the material data of an actual, well-characterized molding compound.[13] The molding compound was an epoxy resin with an extremely high amount of silica filler (ca. 90 wt %) to reduce the coefficient of thermal expansion and curing shrinkage. The side effect of using a high filler content is that the modulus (and, thus, the resulting residual stresses) was relatively high: 28 GPa in the glassy state as compared to about 2.3 GPa for the unfilled material. The material under consideration had a rubbery shear modulus at full curing of $G_2^f = 590$ MPa and a bulk modulus of $K_2^f = 9$ GPa. This meant that the Poisson ratio was $\nu_2^f = 0.468$ and the elongation modulus was $E_2^f = 1732$ MPa, respectively. The curing shrinkage was observed to increase linearly with conversion until a final value of $\varepsilon^{c,\max} = -0.207\%$ (assuming for the coefficients of thermal expansion in the glassy and rubbery state respectively $\alpha_2^G = 11.0\ 10^{-6}$/K, $\alpha_2^R = 31.4\ 10^{-6}$/K). Measurements of the increase in the rubber modulus (G_R) during curing were fitted to the Martin and Adolf model[19]:

$$G_R(\zeta) = G_R^f \left(\frac{\zeta^2 - \zeta_{\text{gel}}^2}{1 - \zeta_{\text{gel}}^2} \right)^{8/3}, \quad \zeta > \zeta_{\text{gel}} \tag{25}$$

where G_R^f is the rubbery modulus in fully cured state, here equal to 590 MPa.

The conversion at gelation was 0.40. The relaxation modulus (G) was approximated with a Havriliak–Negami (HN) type of equation

$$\log G(\zeta, T, \omega) = \log G_R + \frac{\log G_g - \log G_R}{\left[1 + \left(\omega \tau_0 / a_{T,\zeta}\right)^{-m}\right]^n} \tag{26}$$

with as fitting coefficients $\tau_0 = 977$ s, $m = 0.176$, and $n = 2.725$. The curing dependency is captured by the

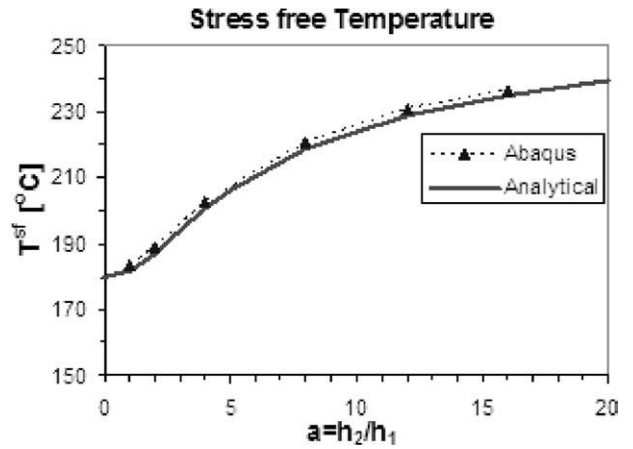

Figure 4 (—) Approximate analytical estimate of the stress-free temperature [Eq. (18)] and (- - -) Abaqus simulation with the full viscoelastic curing-dependent material model.

changing rubbery modulus [Eq. (25)] and a shift factor ($a_{T,\zeta}$) that is curing and temperature dependent:[13]

$$\log a_{T,\zeta} = \log a_T + \log a_\alpha, \tag{27}$$

$$\log a_T = \begin{cases} C_1(T - T_r)/(C_2 + T - T_r) & T > T_c \\ A_1(T - T_c) + A_2 & T \leq T_c \end{cases} \tag{28}$$

$$\log a_\zeta = d_1(1 - \exp[-d_2(1 - \zeta)]) \tag{29}$$

with as coefficients $C_1 = 34.2$, $C_2 = 140.1$ K, $T_r = 120°C$, $A_1 = 0.0281$, $A_2 = -4.059$, $T_c = 102.6°C$, $d_1 = 25.55$, and $d_2 = 1.007$.

In Figure 3, we compare the predictions for the midpoint deflection of a 40 mm long strip for a series of different thickness ratios. This shows that the analytical calculations predicted a maximum deflection (ca. $h_2 = 1.2$ mm), whereas the numerical predictions had a higher maximum at a somewhat larger thickness (h_2). The maximum could be understood from eqs. (21) and (24). For a small thickness ratio, the warpage increased linearly with the thickness ratio [Eq. (21)], whereas for larger thickness ratios, it decreased proportionally to a^2 [Eq. (24)]. The physical interpretation of this effect is that with larger top layer thicknesses, the neutral plane change became important, whereas for small coating thicknesses, it was not.

In the simulations, the isothermal curing was followed by a controlled cooling to room temperature. By extrapolating the warpage versus temperature data to a level where the curvature was zero, we obtained the stress-free temperatures (symbols and dashed line in Fig. 4). These values compared well with those given by Eq. (18). Both the magnitude and shape of the stress-free temperature curve were well reproduced. Figure 5 shows that for this specific case, the curing efficiency factors varied between 0.13 and 0.53. The latter value approached the limiting efficiency value ($f_c^{\max} = 0.60$).

CONCLUSIONS

In this article, we derived simple analytical expressions for predicting the warpage of a structure consisting of an elastic substrate and a curing polymer coating layer. The analysis included the effect of the curing shrinkage and the increase in modulus during curing and neglected viscoelastic effects during curing. A comparison with predictions of numerical models that did not neglect the viscoelasticity during curing showed a perfect agreement; this means that our model was able to capture all of the main effects.

This also showed that it is, in fact, not necessary to know the fully curing-dependent viscoelastic material behavior of the coating to be able to get a good estimate of the effects of the curing shrinkage on residual stresses and warpage. This is of particular practical relevance because the aforementioned material characterization is costly and time consuming and cannot be performed for each new coating material.

In addition to expressions for warpage, we defined a curing shrinkage efficiency factor and obtained an explicit expression for the so-called stress-free temperature. We assume that the theory proposed in this article could be a highly useful tool for predicting the warpage of coatings on thin substrates and for those who are involved in simulating the encapsulation process of microelectronic packages.

References

1. Stoney, G. Proc R Soc London Ser A 1909, 82, 172.
2. Klein, C. J Appl Phys 2000, 88, 5487.
3. Bair, H. E.; Boyle, D. J.; Ryan, C. R.; Taylor, C. R.; Tighe, S. C.; Crouthamel, D. L. Polym Eng Sci 1990, 30, 609.
4. Kim, J., Paik, K.; Oh, S. J Appl Phys 1999, 86, 5474.
5. Klein, C.; Miller, R. J Appl Phys 2000, 87, 2265.
6. Lubin, G. Handbook of Composites; van Nostrand Reinhold: New York, 1982; pp 46, 75.
7. Motahhari, S.; Cameron, J. J Reinforced Plast Compos 1999, 18, 1011.
8. Koganemaru, M.; Ikeda, T.; Miyazaki, N. Microelectron Reliability 2008, 48, 923.
9. Tsai, M.; Chen, Y.; Lee, R. IEEE Trans Compon Pack Technol 2008, 31, 683.
10. Shirangi, M.; Mueller, W.; Michel, B. In Proceedings of the 59th ECTC Conference, San Diego, IEEE, Washington, 2009; p 232.
11. Kelly, G.; Lyden, C.; Lawton, W.; Barret, J.; Saboui, A.; Pape, H.; Peters, H. J. B. IEEE Trans Compon Pack Manuf Technol 1996, 19, 296.
12. Rzepka, S.; Mueller, A. In Proceedings of the 8th EurosimE Conference; IEEE, Piscataway, New Jersey, 2007; p 336.
13. Jansen, K. M. B.; Qian, C.; Ernst, L. J.; Bohm, C.; Kessler, A.; Preu, H.; Stecher, M. Microelectron Reliability 2009, 49, 872.
14. deVreugd, J.; Jansen, K. M. B.; Ernst, L. J.; Bohm, C. Microelectron Reliability 2010, 50, 910.
15. Yan, G.; White, J. Polym Eng Sci 1999, 39, 1856.
16. Saraswat, M. K.; Jansen, K. M. B.; Ernst, L. J. In Proceedings of 1st ESTC Conference, Dresden; IEEE, Piscataway, New Jersey, 2006; p 782.
17. Yang, D. G.; Jansen, K. M. B.; Ernst, L. J. Microelectron Reliability 2007, 47, 310.
18. Hwang, S. J.; Chang, Y. S. IEEE Trans Compon Pack Technol 2006, 29, 112.
19. Adolf, D. B.; Martin J. E.; Chambers, R. S.; Burchett, S. N.; Guess, T. R. J Mater Res 1998, 13, 530.